

G. Pintsuk et al.

# Manufacturing and Characterization of PIM-W Materials as Plasma Facing Materials

(18th May 2015 – 22nd May 2015)  
Aix-en-Provence, France

“This document is intended for publication in the open literature. It is made available on the clear understanding that it may not be further circulated and extracts or references may not be published prior to publication of the original when applicable, or without the consent of the Publications Officer, EUROfusion Programme Management Unit, Culham Science Centre, Abingdon, Oxon, OX14 3DB, UK or e-mail [Publications.Officer@euro-fusion.org](mailto:Publications.Officer@euro-fusion.org)”.

“Enquiries about Copyright and reproduction should be addressed to the Publications Officer, EUROfusion Programme Management Unit, Culham Science Centre, Abingdon, Oxon, OX14 3DB, UK or e-mail [Publications.Officer@euro-fusion.org](mailto:Publications.Officer@euro-fusion.org)”.

The contents of this preprint and all other EUROfusion Preprints, Reports and Conference Papers are available to view online free at <http://www.euro-fusionscipub.org>. This site has full search facilities and e-mail alert options. In the JET specific papers the diagrams contained within the PDFs on this site are hyperlinked.

# Manufacturing and Characterization of PIM-W Materials as Plasma Facing Materials

G Pintsuk<sup>1,\*</sup>, S Antusch<sup>2</sup>, M Rieth<sup>2</sup> and M Wirtz<sup>1</sup>

<sup>1</sup>Forschungszentrum Juelich GmbH, 52425 Juelich, Germany

<sup>2</sup>Karlsruhe Institute of Technology (KIT), Institute for Applied Materials, 76344 Eggenstein-Leopoldshafen, Germany

E-mail: g.pintsuk@fz-juelich.de

PACS: 28.52.-s, 28.52.Fa, 65.40.De

**Abstract.** Powder Injection Molding (PIM) was used to produce pure and particle reinforced W materials to be qualified for the use as plasma facing material (PFM). As alloying elements  $\text{La}_2\text{O}_3$ ,  $\text{Y}_2\text{O}_3$ , TiC, and TaC were chosen with a particle size between 50 nm and 2.5  $\mu\text{m}$ , depending on the alloying element. The fabrication of alloyed materials was done for different compositions using powder mixtures. Final sintering was performed in  $\text{H}_2$  atmosphere at 2400 °C resulting in plates of  $55 \times 22 \times 4 \text{ mm}^3$  with ~98 % theoretical density.

The qualification of the materials was done via high heat flux testing in the electron beam facility JUDITH-1. Thereby, ELM-like 1000 thermal shock loads of  $0.38 \text{ GW/m}^2$  for 1 ms and 100 disruption like loads of  $1.13 \text{ GW/m}^2$  for 1 ms at a base temperature of 1000 °C were applied. The obtained damage characteristics, i.e. surface roughening and crack formation, were qualified versus an industrially manufactured pure reference tungsten material and linked to the materials microstructure and mechanical properties.

## 1. Introduction

1    Within the framework of the EUROfusion Consortium, high heat flux materials development for the  
2    first wall of a DEMO reactor and in particular for the high heat flux regions of the divertor is one key  
3    topic. Thereby, the focus for the plasma facing materials was in the past [1] and still is strongly set on  
4    tungsten and tungsten-based materials. Tungsten-based materials are attractive to be used in various  
5    applications for fusion power plants. Besides its advantages, the main drawbacks are its brittleness and  
6    correlated difficult machinability as well as the narrow range of possible alloys using the commercial  
7    fabrication route. In addition, the semi-finished products are limited to plates and rods. These issues are  
8    addressed by the development and fabrication of complex near-net shaped tungsten parts via Powder  
9

10 Injection Molding (PIM), which also allows the joining of different materials without brazing and a  
11 rapid development of new tungsten materials [2, 3].

12 The R&D on new tungsten materials aims to improve its resistance to operational loads, i.e. thermal  
13 shock and thermal shock induced thermal fatigue loads mainly due to ELMs [4-8] and pure thermal  
14 fatigue loads during steady state heat loading [9, 10]. While the resistance to ELMs is a purely material  
15 dependent issue, the resistance to steady state heat loads also strongly depends on the component design.  
16 In this work the focus is set on the development of materials with an increased resistance to ELMs.  
17 Therefore, various particle reinforced PIM-W materials with the alloying elements  $\text{La}_2\text{O}_3$ ,  $\text{Y}_2\text{O}_3$ , TiC,  
18 and TaC were manufactured using powder mixtures of commercially available powders.

19 Characterization of the materials was performed determining the materials microstructure and hardness  
20 and by performing high heat flux testing in the electron beam facility JUDITH-1 [11]. Thereby, ELM-  
21 like 1000 thermal shock loads of  $0.38 \text{ GW/m}^2$  for 1 ms at a base temperature of  $1000 \text{ }^\circ\text{C}$  were applied.  
22 These application relevant conditions are slightly above the damage threshold for commercial reference  
23 tungsten grades, allowing the qualification of the individual materials towards this reference material.  
24 Based on this pre-qualification, disruption like tests with 100 pulses at  $1.13 \text{ GW/m}^2$  for 1 ms and at  $1000$   
25  $^\circ\text{C}$  base temperature were performed on selected materials (pure W, W-2 $\text{Y}_2\text{O}_3$ , W-1TiC, W-2TaC). In all  
26 cases, the damage quantification was done by post-mortem examinations using metallographic means.

27

## 28 **2. Materials - manufacturing and microstructure**

### 29 *2.1. PIM: used powders, powder mixtures and feedstock preparation*

30 The average particle size distribution of the used tungsten powder was in the range of 1.0 to 2.0  $\mu\text{m}$   
31 Fisher Sub-Sieve Size (FSSS). As doping materials  $\text{La}_2\text{O}_3$  (FSSS < 2.50  $\mu\text{m}$ ),  $\text{Y}_2\text{O}_3$  (FSSS < 1.50  $\mu\text{m}$ ),  
32 TiC (FSSS < 50 nm), and TaC powders (FSSS < 1.0  $\mu\text{m}$ ) were used. These individual powders were  
33 mixed with pure tungsten to obtain various powder compositions defined by wt.-%: pure W with two  
34 different powder mixtures (W-170, W-5050), W-2 $\text{La}_2\text{O}_3$ , W-0.5/1/2 $\text{Y}_2\text{O}_3$ , W-1/1.5/2/3TiC, and W-  
35 0.5/1/2TaC.

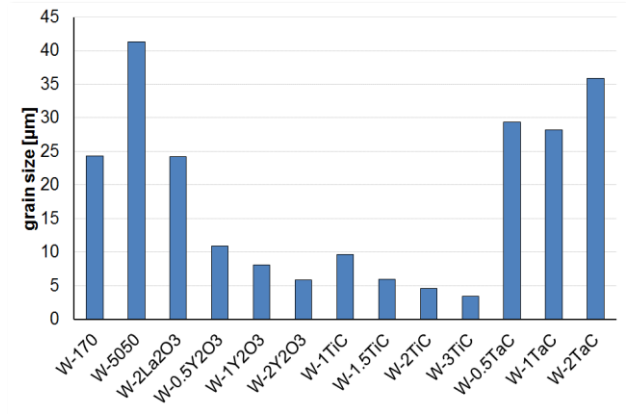
36 After a heat treatment at 80 °C for moisture removal, the powders were dry mixed to form the  
37 “feedstock” with a 50 vol.-% binder system in a kneader. The finished granulated feedstock was  
38 homogeneous and free from agglomeration.

39

#### 40 2.2. *PIM: production of plates and microstructure*

41 The injection molding of the “green parts” (consisting of powder and binder) was carried out on an  
42 ELEKTRA injection molding machine. After injection molding the green parts were debound. During  
43 the debinding step not only binder and impurities (mainly O and C) were removed, but also the high  
44 residual stresses generated during injection molding were released. Finishing of the plates was done in  
45 a subsequent sintering process in dry H<sub>2</sub> for 2 h. The finished plates (Figure 1) are characterized by a  
46 shrinkage of nearly 20 % during the heat-treatment process and achieve ~ 98 % T.D after sintering at  
47 2400 °C.

48 The materials microstructure is in all cases isotropic, but varies among the different material  
49 compositions strongly with regard to their average grain size (figure 1). The smallest grains were found  
50 for Y<sub>2</sub>O<sub>3</sub> and TiC doped materials, for which the average grains size is, depending on the composition,  
51 only by a factor 2 to 7 larger than the original size (average: 1.5 μm) of the W-powder. This suggests  
52 that these materials should be also highly recrystallization resistant. All other materials exhibit an  
53 increase in grain size by more than a factor 16. In particular, for the TaC doped materials this result is  
54 surprising as a similar performance to TiC additions would have been expected, even if larger particle  
55 sizes were used (see section 2.1). For the La<sub>2</sub>O<sub>3</sub> doped material it has to be stated that the sintering  
56 temperature was above the melting temperature of La<sub>2</sub>O<sub>3</sub> and in the microstructural analysis no La<sub>2</sub>O<sub>3</sub>  
57 was found, but very clean grain boundaries with regard to impurities.



58

59 Figure 1: Finished plate with dimensions of  $55 \times 22 \times 4 \text{ mm}^3$  and a weight of  $\sim 75 \text{ g}$ ; average tungsten  
60 grain size of the produced PIM-W materials.

61

### 62 2.3. Reference material

63 The reference material is pure tungsten grade (IGP W) with a purity of 99.97 wt% manufactured by the  
64 Plansee AG, Austria, according to the ITER material specification. The forged rod was produced with  
65 the dimensions  $36 \times 36 \times 480 \text{ mm}^3$  and was exposed to a stress relieving treatment by thermal annealing  
66 after the production process. Due to the production process the grain structure is strongly anisotropic  
67 with needle like grains parallel to the forging direction ( $\varnothing = 5 - 10 \text{ μm}$ , length ca.  $25 \text{ μm}$ ). In its  
68 recrystallised state ( $1600 \text{ °C}$  for 1 h) the materials loses its pronounced elongated grain structure and  
69 experiences grain growth with an average grain size of about  $64 \text{ μm} \times 102 \text{ μm}$ .

70

## 71 3. Experiments

72 The simulation of transient thermal shocks was done with the electron beam device JUDITH-1 at  
73 Forschungszentrum Jülich [JUDI] on small-scale samples. These samples were prepared via electrical  
74 discharge machining (EDM) from the PIM-materials with dimensions of  $10 \times 10 \times 4 \text{ mm}^3$ . In  
75 comparison, due to the anisotropic microstructure, the tests on the reference W-grade were performed  
76 on specimens from the stress-relieved material in two different orthogonal orientations (elongated grains  
77 parallel and perpendicular to the loaded surface), both with dimensions of  $12 \times 12 \times 5 \text{ mm}^3$ . Similar  
78 sized specimens were tested for the recrystallized material only in one orientation. The final preparation  
79 of the specimens was done by polishing the surface to a mirror finish. This allows obtaining well defined

80 starting conditions, in particular in view of expected surface damage, i.e. roughening and crack  
81 formation.

82 The chosen testing conditions were based on experience with other tungsten materials and in view of  
83 relevant operational scenarios in a fusion reactor. Therefore, for the ELM-like loading an absorbed  
84 power density of 0.38 GW/m<sup>2</sup> (taking an electron absorption coefficient of 0.55 into account) a pulse  
85 duration of 1 ms, a pulse number of 1000, and a base temperature of 1000 °C was chosen. These  
86 conditions are expected to be above the expected damage threshold of the materials to allow  
87 quantification of the damage and qualification of the material. Furthermore, applying 1000 pulses  
88 addresses the influence of thermal fatigue on the damage behavior. Based on this qualification,  
89 disruption like tests with 100 pulses at 1.13 GW/m<sup>2</sup> for 1 ms and at 1000 °C base temperature were  
90 performed on selected materials (pure W, W-2Y<sub>2</sub>O<sub>3</sub>, W-1TiC, W-2TaC). The exposed area for all tests is  
91 4 × 4 mm<sup>2</sup> with a focused electron beam (∅ ~1 mm) at very high frequencies (40 kHz in x-direction and  
92 31 kHz in y-direction). The repetition frequency was < 1 Hz and defined by requirement to allow a cool  
93 down back to base temperature.

94 After the exposure in JUDITH-1, the induced surface damage was investigated by SEM, determining  
95 the amount of crack formation, and laser profilometry for quantification of the surface roughness.  
96 Subsequently, the cross sections of the samples were investigated by metallographic means in order to  
97 analyse particularly crack propagation into the bulk material. Supporting experiments were done by  
98 measuring the materials Vickers hardness (HV1; max. load of the indenter: 2 N) and for a few materials  
99 also the stress-strain behavior via 4-pt. bending tests between RT and 400 °C. The latter were done with  
100 a strain rate of 0.033 mm/min on 12 × 1 × 1 mm<sup>3</sup> specimens.

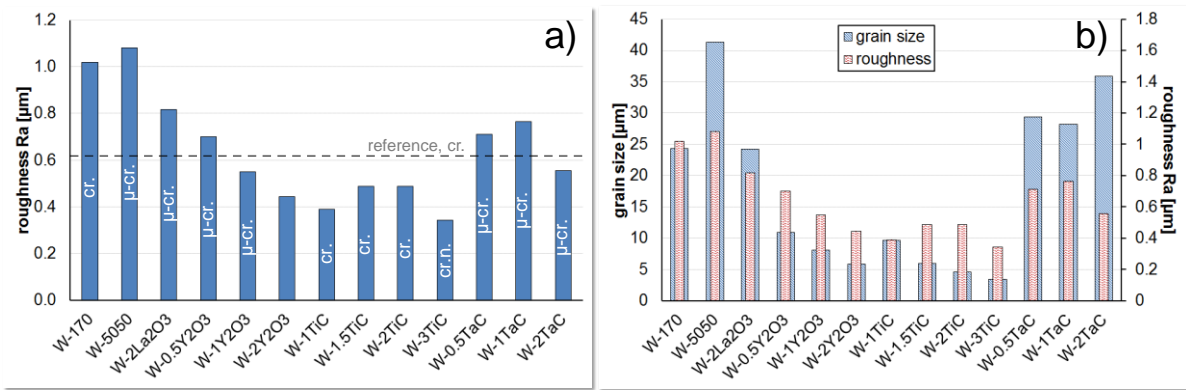
101

#### 102 **4. Results**

103 When dealing with thermal fatigue induced surface damage due to ELM-like loading conditions, a clear  
104 indicator of the amount of plastic deformation is the surface roughness. Based on an original value of  
105  $R_a = 0.08\text{-}0.1\ \mu\text{m}$  for the mirror like surface of the specimens, the surface roughness increased for all  
106 specimens (figure 2a). In comparison to the reference material, characterized by a roughness of ~0.6 μm  
107 in its stress relieved state, part of the Y<sub>2</sub>O<sub>3</sub> doped and the TiC-doped materials showed a better

108 performance, i.e. lower surface roughness. Taking the performance of the recrystallized reference  
 109 material into account ( $R_a = 1.33 \mu\text{m}$ ), all PIM-W grades showed an improved performance. One factor  
 110 thereby is the material's grain size, as indicated in figure 2b. By correlating grain size and obtained  
 111 surface roughness a clear tendency is found that, within certain variations, smaller grains also result in  
 112 a reduced amount of surface roughening.

113



114

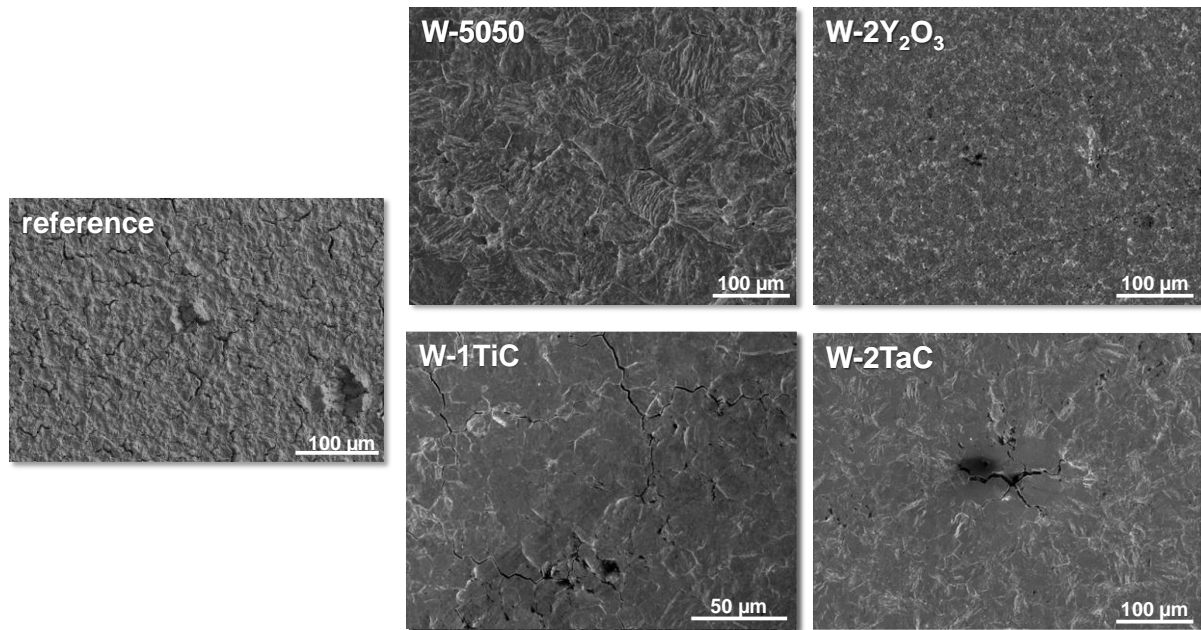
115 Figure 2: Determined roughness of the PIM-W materials a) in relation to the reference material (stress  
 116 relieved; recrystallized:  $R_a = 1.33 \mu\text{m}$ ) including observed crack formation ( $\mu$ -cracks, cracks and crack  
 117 network) and b) in relation to the materials grain size

118

119 In addition to surface roughening, for almost all tested PIM materials, except W-2Y<sub>2</sub>O<sub>3</sub>, the loaded  
 120 surface was characterized by thermal fatigue induced crack formation. This was ranging from  $\mu$ -cracks  
 121 in areas of local inhomogeneity or at grain boundary triple junctions to crack formation along grain  
 122 boundaries and formation of crack networks (figure 2a). The penetration of the cracks towards the bulk  
 123 is limited to a few tens  $\mu\text{m}$  in the worst case, which is based on the lack of materials brittleness at the  
 124 chosen base temperature and the still comparably low number of pulses [7, 8]. In correlation, for the  
 125 reference material shallow cracking along grain boundaries but no crack network formation was found,  
 126 which is shown in figure 3 in relation to the PIM materials with the best performance for a certain  
 127 material composition / particle reinforcement.

128





129

130 Figure 3: SEM images of the loaded surface: comparison between the reference tungsten grade with  
 131 grains perpendicular to the loaded surface (stress relieved) to the materials with the best performance  
 132 for a particular particle reinforcement

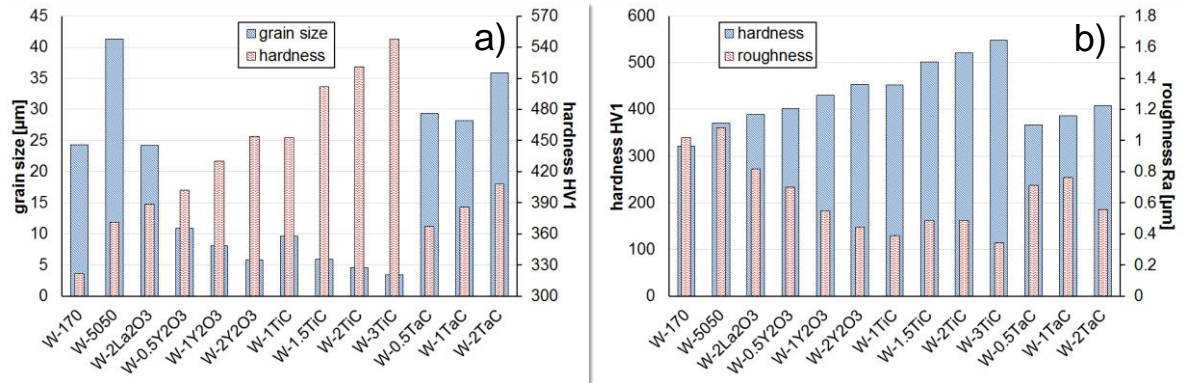
133

134 Besides the above mentioned correlation between grain size and surface roughening, there seems to be  
 135 also a link between the former and the mechanical properties of a material. By measuring the material's  
 136 hardness as an indicator for the material's strength, figure 4 shows that a decreasing grain size and  
 137 accordingly a decreasing surface roughness is directly related to an increase in hardness. By comparison  
 138 to the reference material (stress relieved, 445 HV1), only the TiC-doped materials with particle additions  
 139 of  $\geq 1.5$  wt.% exhibit a significant increase in hardness while the hardness for W-1TiC and the best  
 140 performing PIM-W grade W-2Y<sub>2</sub>O<sub>3</sub> is in the same range as the one for the reference material. For all  
 141 other W-grades, i.e. the pure W and W-TaC doped materials, hardness values were obtained in the  
 142 proximity of those for the recrystallized reference material (355 HV1).

143 In related 4pt.-bending tests of the PIM-W grades shown in figure 3, pure W and W-2TaC performed  
 144 similar with regard to yield and bending strength and in particular pure W showed already some ductility  
 145 at 100 °C. In contrast, W-1TiC and W-2Y<sub>2</sub>O<sub>3</sub> showed ductile behavior first at 200 °C and 300 °C,  
 146 respectively, but with a significantly higher yield and bending strength, which is at 300 °C for W-1TiC  
 147 and W-2Y<sub>2</sub>O<sub>3</sub> about 3.5 and 5.5 times larger, respectively, than those for pure W (~200 MPa). In

148 comparison to reference tungsten, on which tensile tests were performed with a deformation speed of  
 149 0.2 mm/min, the yield strength was about 550 MPa [12].

150

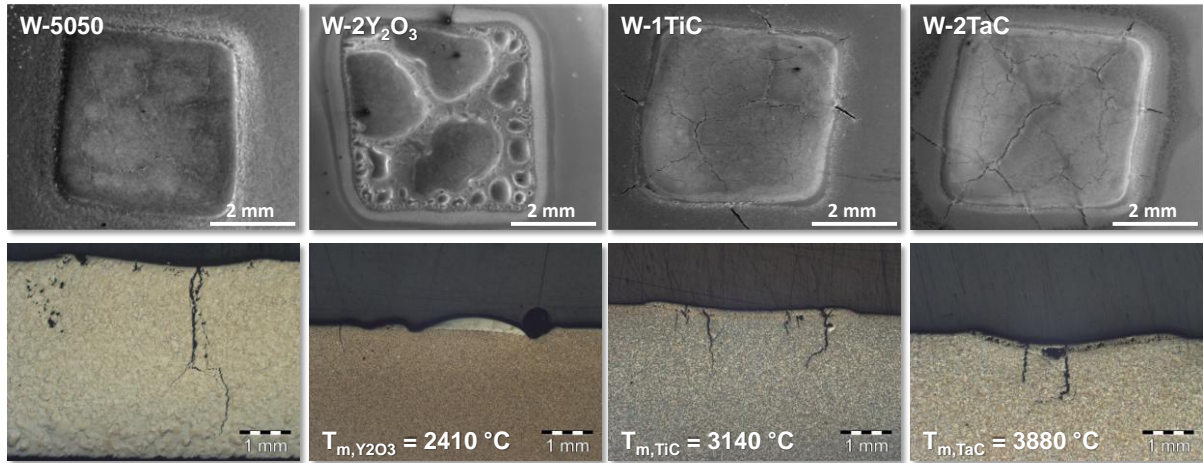


151

152 Figure 4: Hardness of the PIM-W materials in relation to a) the grain size and b) the surface roughness  
 153 after thermal shock; hardness of reference material: 445 HV1 and 355 HV1 in the stress relieved and  
 154 recrystallized state, respectively

155

156 In contrast to ELM-like loading, during disruption like testing the melting threshold of the material is  
 157 exceeded. This results for the four investigated materials in either homogeneous (pure W, W-1TiC and  
 158 W-2TaC) or inhomogeneous (W-2Y<sub>2</sub>O<sub>3</sub>) molten and resolidified structures (figure 5). The reason for the  
 159 inhomogeneous melting might be related to the comparably low melting temperature and binding energy  
 160 for Y<sub>2</sub>O<sub>3</sub> compared to TiC and TaC and the increased probability for the formation of tungsten oxides.  
 161 Furthermore, large and, despite of the high base temperature, kind of brittle crack formation was found  
 162 for those materials exhibiting homogeneous melting with a crack depth of up to several mm. In case of  
 163 W-1TiC and W-2TaC, these cracks were not limited to the molten area but also protruded towards the  
 164 non-loaded but, due to lateral heat transfer, heat affected zone surrounding the loaded spot.



165

166 Figure 5: SEM images of the surface (top) and LM images of the cross sections (bottom) after disruption  
 167 like loads ( $P_{\text{abs}} = 1.13 \text{ GW/m}^2$ ,  $\Delta t = 5 \text{ ms}$ ,  $n = 100$ ,  $T = 1000 \text{ }^\circ\text{C}$ )

168

169 **5. Summary**

170 For the qualification of new W-grades manufactured via PIM, the materials were subjected to 1000 and  
 171 100 pulses of ELM and disruption like loading conditions, respectively, in the electron beam facility  
 172 JUDITH-1. The results for ELM-like tests have shown that the occurring thermal fatigue damage, i.e.  
 173 roughening and crack formation, is depending on the grain size of the material and the correlated  
 174 mechanical properties. Lower grain sizes and therefore higher hardness / mechanical strength results in  
 175 decreased roughening and therefore an increased resistance to thermal fatigue damage in view of the  
 176 expected number of ELM pulses in ITER and beyond. Accordingly, economically viable W-materials  
 177 with  $\text{Y}_2\text{O}_3$  ( $< 1.50 \mu\text{m}$ ) and  $\text{TiC}$  ( $< 50 \text{ nm}$ ) content that have been produced by using standard  
 178 industrially available powders, have shown an improved performance compared to a reference  
 179 industrially manufactured tungsten grade fulfilling the ITER requirements. In contrast, W reinforced  
 180 with  $\text{TaC}$  ( $< 1.0 \mu\text{m}$ ) particles performed similar to the reference while pure W exhibited similar  
 181 properties and results as the reference material after recrystallization.

182 The results for the disruption like tests have shown, that melting, melt motion and crack formation is  
 183 related to the added particle reinforcement. Thereby,  $\text{Y}_2\text{O}_3$  doped materials have shown inhomogeneous  
 184 melting and resolidification but hardly any crack formation while all other materials are characterized  
 185 by homogeneous melting with strong crack formation up to several mm depth. A decisive role seems to

186 play the melting temperature and binding energy. In view of the performance in a tokamak and with  
187 regard to the qualification of Y<sub>2</sub>O<sub>3</sub> and TiC doped W-materials further investigations are needed to  
188 determine if extensive crack formation or inhomogeneous melting poses the higher risk for plasma  
189 operation and component lifetime.

190

## 191 **6. Acknowledgement**

192 This work has been carried out within the framework of the EUROfusion Consortium and has received  
193 funding from the Euratom research and training programme 2014-2018 under grant agreement No  
194 633053. The views and opinions expressed herein do not necessarily reflect those of the European  
195 Commission or those of the European Commission.

196

197

## 198 **7. References**

- 199 [1] Rieth M, Dudarev S L, Gonzalez de Vicente S M, Aktaa J, Ahlgren T, Antusch S, Armstrong D E  
200 J, Balden M, Baluc N, Barthe M-F, Basuki W W, Battabyal M, Becquart C S, Blagoeva D,  
201 Bodyryeva H, Brinkman J, Celino M, Ciupinski L, Correia J B, De Backer A, Domain C,  
202 Gaganidze E, Garcia-Rosales C, Gibson J, Gilbert M R, Giusepponi S, Gludovatz B, Greuner H,  
203 Heinola K, Höschen T, Hoffman A, Hostein N, Koch F, Krauss W, Li H, Lindig S, Linke J,  
204 Linsmeier Ch, Lopez-Ruiz P, Maier H, Matejicek J, Mishra T P, Muhammed M, Munoz A, Muzyk  
205 M, Nordlund K, Nguyen-Manh D, Opschoor J, Ordas N, Palacios T, Pintsuk G, Pippan R, Reiser  
206 J, Riesch J, Roberts S G, Romaner L, Rosinski M, Sanchez M, Schulmeyer W, Traxler H, Urena A,  
207 van der Laan J G, Veleva L, Wahlberg S, Walter M, Weber T, Weitkamp T, Wurster S, Yar M A,  
208 You J H, Zivelonghi A 2013 *Journal of Nuclear Materials* **432**, Issues 1-3, 482
- 209 [2] Antusch S, Commin L, Heneka J, Piotter V, Plewa K, Walter H 2013 *Fusion Engineering and*  
210 *Design* **88**, Issues 9-10, 2461
- 211 [3] Antusch S, Commin L, Mueller M, Piotter V, Weingaertner T 2014 *Journal of Nuclear Materials*  
212 **447**, Issues 1-3, 314
- 213 [4] Linke J 2006 *Fusion Science and Technology* 49 455

- 214 [5] Pintsuk G, Prokhodtseva A, Uytendhouwen I 2011 *Journal of Nuclear Materials* **417** 481-486
- 215 [6] Pintsuk G, Loewenhoff Th 2013 *Journal of Nuclear Materials* **438** S945
- 216 [7] Loewenhoff T, Bürger A, Linke J, Pintsuk G, Schmidt A, Singheiser L, Thomser C 2011 *Physica*  
217 *Scripta* **T145** 014057
- 218 [8] Loewenhoff Th, Linke J, Pintsuk G, Thomser C 2012 *Fusion Engineering and Design* **87**, Issues  
219 **7-8**, 1201
- 220 [9] Pintsuk G, Bednarek M, Gavila P, Gerzosovitz S, Linke J, Lorenzetto P, Riccardi B, Escourbiac  
221 F, 2015 *Fusion Engineering and Design*, in press (doi:10.1016/j.fusengdes.2015.01.037)
- 222 [10] Pintsuk G, Bobin-Vastra I, Constans S, Gavila P, Rödiger M, Riccardi B 2013 *Fusion Engineering*  
223 *and Design* **88**, Issues **9-10**, 1858
- 224 [11] Duwe R, Kuehnlein W, Muenstermann H 1995 *Fusion Technology* 1994 355
- 225 [12] -Wirtz M, Linke J, Loewenhoff Th, Pintsuk G, Uytendhouwen I, this conference